Carbohydrate Polymers 106 (2014) 109–120

Contents lists available at ScienceDirect

Carbohydrate Polymers

journal homepage: www.elsevier.com/locate/carbpol

Controlled release of tinidazole and theophylline from chitosan based composite hydrogels

Himadri Sekhar Samanta, Samit Kumar Ray*

Department of Polymer Science and Technology, University of Calcutta, 92, A.P.C. Road, Kolkata 700009, India

ARTICLE INFO

Article history:
Received 11 December 2013
Received in revised form 22 January 2014
Accepted 28 January 2014
Available online 5 February 2014

Keywords:
Chitosan
Polyacrylic acid
Composite hydrogels
Synthesis
Characterization
Drug release

ABSTRACT

Several composite hydrogels were synthesized by free radical crosslink copolymerization of acrylic acid (AA) and N′ methylene bis-acrylamide (MBA) in the presence of chitosan (CS). During polymerization CS was incorporated in situ in the crosslinked polyacrylic acid gel to produce composite hydrogels. The structure and properties of the hydrogels were characterized by FTIR, ^{13}C NMR, DTA–TGA, XRD, swelling and diffusion characteristic and also network parameters. The loading and the in vitro release behaviours of theophylline and tinidazole model drugs were studied with these hydrogels. The wt% of CS and MBA and pH of the medium was found to strongly influence the drug release behaviour of the gels. Accordingly, the release rate of these two drugs was much faster at pH of 7.6 than at pH 1.5.

1. Introduction

Most of the hydrogels are widely used as drug carrier because of its high swelling in water, soft pliable nature, biocompatibility and biodegradability. It can absorb large quantities of water or physiological solutions while the absorbed solutions are not removable even under pressure. In the swollen state, these gel networks become soft and rubbery, resembling a living tissue. No additional treatment is required for removal of these biodegradable delivery systems after end use (Bertza et al., 2013). These smart polymers are obtained by covalent crosslinking or non-covalent crosslinking of natural or biocompatible synthetic polymers (Islam & Yasin, 2012). Natural polymers are abundant and thus less expensive. Further, these polymers are non-toxic, biocompatible and biodegradable. However, hydrogels based on natural polymer are of poor mechanical strength (Ahn, Choi, & Cho, 2001; Lorenzo, Fernandez, Puga, & Concheiro, 2013). On the other hand most of the hydrogels based on synthetic polymers are mechanically durable but not biodegradable. Further, these synthetic hydrogels are expensive and also vulnerable to shear degradation (Sionkowska, 2011). Thus, hydrogels made by combining biocompatible synthetic polymers like various acrylic polymers with natural or semi-synthetic biopolymers based on polysaccharides or proteins have been widely explored to achieve high concentration of drugs in the specific region or tissue and the controlled release profile for extended time periods (Bertza et al., 2013; Matricardi, Meo, Coviello, Hennink, & Alhaique, 2013; Zhou, Zhang, Zhang, & Chen, 2011). For preparing gel a natural polymer and a synthetic polymer may be combined by some chemical reactions like grafting of a synthetic polymer on a natural polymer (Sokker, Abdel Ghaffar, Gad, & Aly, 2009; Zhang, Wang, & Wang, 2007), IPN formation by crosslinking one or both polymers (Yanga, Chena, Pana, Wanc, & Wang, 2013; Yue, Sheng, & Wang, 2009; Zhang et al., 2007), semi-IPN microspheres blend formation from natural and synthetic polymers such as polyvinyl alcohol and hydroxyethyl cellulose (Sullad, Manjeshwar, & Aminabhavi, 2010a, 2010b), gelatin and hydroxyethyl cellulose (Kajjari, Manjeshwar, & Aminabhavi, 2011) by emulsion crosslinking, in situ polymerization of a monomer in the presence of a natural polymer, etc. (Samanta & Ray, 2014). In grafting the synthetic monomer in small quantity is allowed to polymerize in the matrix of a base or trunk polymer where the monomer polymerize as well as form chemical bond with the base polymer. Free radicals are also generated on the base polymer and the macroradicals take part in graft copolymerization with the monomer. Crosslinking also occurs by formation of chemical bonds among macroradicals of the base polymer (Panic, Madzarevic, Husovic, & Velickovic, 2013; Wang & Wang, 2010). For producing a stable gel network there should be a good balance of grafting and crosslinking. However, highly reactive macroradicals or monomer radicals like acrylic radicals cause more of grafting and homopolymerization than crosslinking (Bhattacharya, Rawlins, & Ray, 2009). Further, the base polymer in a graft copolymerization is selective only to a

* Corresponding author. Fax: +91 33 23508386.
E-mail address: samitcu2@yahoo.co.in (S.K. Ray).

0144-8617/$ – see front matter © 2014 Elsevier Ltd. All rights reserved.
http://dx.doi.org/10.1016/j.carbpol.2014.01.097

specific number of monomers. Another way of combining a natural and synthetic polymer is to polymerize small amount of a synthetic monomer in aqueous solution of a natural polymer. However, for free radical solution polymerization, total monomer concentration in water should be at least 15–20 wt% (Samanta & Ray, 2014) while it is difficult to make an aqueous solution of a natural polymer with polymer concentration >5 wt% because of its high molecular weight and thus high viscosity of the solution. Thus, modifying a hydrogel of a natural polymer with a synthetic polymer by in situ polymerization of small amount of a synthetic monomer is difficult. Hence, semi- and full IPN type composite hydrogels are made by in situ incorporation of a natural polymer in the polymerization reaction mixtures of synthetic monomers. Accordingly, in the present work CS was incorporated in polyacrylic acid gel by in situ incorporation during crosslink copolymerization of acrylic acid and MBA in water. Acrylic acid monomer was chosen since its polymer viz. polyacrylic acid (PAA) is a pH responsive polyelectrolyte which has been extensively used for drug delivery to specific sites of gastrointestinal tract (Ahn et al., 2001). However, extensive swelling of uncrosslinked PAA in water limits its applications in drug delivery because of its dissolution before delivery of drug (Ahn et al., 2001). Thus, in the present work PAA was crosslinked with comonomer crosslinker MBA and subjected to interpenetration with CS for achieving stable network of a gel. MBA was chosen because of its use in drug delivery systems (Jameela, Lakshmi, James, & Jayakrishnan, 2002; Samanta & Ray, 2014). Among the various natural polymers CS was chosen because of its high molecular weight, high charge density and mucoadhesive properties leading to its wide spread use in drug delivery systems (Rao, Naidu, Subha, & Aminabhavi, 2006; Rokhade, Shelke, Patil, & Aminabhavi, 2007). In PAACS composite gel apart from crosslinking of PAA, a polyelectrolyte complex is also formed by electrostatic interaction of cationic CS and anionic PAA which increases further the stability of the gel. The hydrogels made from CS and PAA have also been reported by many researchers. A novel hydrogel made from CS, PAA and attapulgite was reported to show high swelling in water (Zhang et al., 2007). Torre et al. prepared hydrogel of CS and PAA by blending these two polymers in aqueous acetic acid solution followed by freeze drying to produce the network without any chemical crosslinking and amoxicillin drug was incorporated in situ in the blend network (Paloma, Torrea, Enobakharea, Torradob, & Torrado, 2003). Ahn et al. carried out template polymerization of acrylic acid in the presence of CS by UV radiation and this polyelectrolyte hydrogel was reported for transmucosal drug delivery system (Ahn et al., 2001). In a similar way, Shim and Nho prepared CS-PAA hydrogel without any chemical crosslinker by gamma radiation and this hydrogel was reported for release of 5-fluorouracil drug (Shim & Nho, 2003).

From the above discussion it is evident that hydrogels based on CS and PAA have been widely used for study of drug release. However, in these studies hydrogels were prepared either by blending PAA and CS or polymerizing acrylic acid in the presence of CS by UV or gamma radiations. In these gels no chemical crosslinkers have been used and stability of these gels depends on freeze drying and formation of polyion complexes between cationic CS (due to its NH_3^+ group) and anionic PAA. In the present work several hydrogels have been prepared by crosslink copolymerization of varied amounts of acrylic acid and MBA for obtaining stable gel networks. In these hydrogels varied concentrations of CS were incorporated in situ during polymerization and the resulting composite hydrogels were used for release of two important drug viz. tinidazole and theophylline. Tinidazole or 1-(2-ethylsulfonylethy)-L-2-methyl-5 nitroimidazole drug is mainly used for treatment of intestinal amoebiasis and other colon infections and also for periodontitis. However, this synthetic antibiotic has some potential hazards like peripheral neuropathy and convulsive seizures (Tracy & Webster, 1996). Thus, effective release of low dosage of this drug at colon using a colon targeted specific drug delivery system is desirable (Krishnaiah, Bhaskarreddy, Satyanarayana, & Karthikeyan, 2002). Because of good solubility in acidic medium, this drug is also expected to have good solubility in the present mucoadhesive PAACS hydrogel. Similarly, theophylline is a methylxanthine drug used as a bronchodialator for treatment of asthma and chronic obstructive pulmonary disease (COPD) by oral or intravenous route. However, clinical use of this drug is limited because of its adverse effects like nausea, vomiting, tachycardia, headache, seizure and agitation (Mastiholimath, Dandagi, Jain, Gadad, & Kulkarni, 2007). Thus, sustained delivery of the required concentration of the drug using a polymer hydrogel like the present PAA-CS composite gel would eliminate the side effects of the drug. Thus, in the present work the PAA-CS hydrogels were used for study of sustained release of these two important model drugs.

2. Materials and methods

2.1. Materials

Chitosan (CS) was kindly donated as free sample by Indian Sea Food, Cochin. It was used without any further purification. The comonomer crosslinker N,N′-methylene bisacrylamide (MBA, from Merck) and the redox pair of initiators ammonium persulfate (APS, from Fluka) and sodium metabisulfite were of analytical grade and used without any further purification. The monomer acrylic acid (AA, Merck) was used after vacuum distillation. The drugs theophylline and tinidazole were purchased from Loba Chemicals, Mumbai, India and used as obtained.

2.2. Methods

2.2.1. Preparation of hydrogel

At first PAA gels were prepared at varied initiator, total monomer (AA), crosslinker (MBA) concentration in a three necked reactor placed on a constant temperature bath and fitted with a stirrer, a thermometer pocket and a condenser at 30 °C. For preparing composite gel varied concentrations, i.e., 0.5, 1.0 and 2.0 wt% of CS was made in deionized water containing 2 wt% of acetic acid in a 250 mL glass beaker by gradual addition of required amount of CS to obtain a viscous solution of CS. The required amount of CS solution and AA monomer was then poured into the reactor. Temperature was maintained at 30 °C and aqueous solution of initiators was added to the reactor followed by the addition of MBA (crosslinker). After polymerization the reaction mixture was cooled to ambient temperature. Hydrogel obtained was cut into small blocks and then immersed into double distilled water for 48 h to remove water soluble oligomer, uncrosslink polymer and unreacted monomers from the gel. The gel obtained was dried in a vacuum oven at 60 °C to a constant weight. The dried gel, also called xerogel was then disintegrated in a blender.

2.2.2. Yield, sol and gel content of the hydrogel

The hydrogels as prepared above were first dried to a constant weight (m_c) in a vacuum oven and then it was taken in water and kept for a week with occasional shaking to remove the water soluble part from the hydrogel. The water insoluble gel sample was further dried (xerogel) in vacuum oven to a constant weight (m_d). Yield, gel and sol% was obtained as

$$\text{Yield\%} = \frac{m_c}{m_i} \times 100 \quad (1)$$

$$\text{Gel\%} = \frac{m_d}{m_c} \times 100 \quad (2)$$

$$\text{Sol\%} = 100 - \text{Gel\%} \quad (2a)$$

where m_i is total weight of monomers (acrylic acid and MBA) and CS used for synthesis of gel.

2.3. Characterization of the hydrogels

2.3.1. Fourier transform infrared (FTIR) spectroscopy

FTIR spectra of the drug free and drug loaded hydrogel samples were recorded on a FTIR spectrometer (Perkin Elmer, model-Spectrum-2, Singapore) using KBr pellet made by mixing KBr with fine powder of the drug free and drug loaded gel samples (10:1 mass ratio of KBr to polymer, for only drug sample 50:1 ratio of KBr to drug was used).

2.3.2. ^{13}C (nuclear magnetic resonance, NMR) spectra

^{13}C NMR spectra of the CS and PAA-CS composite gel samples were taken on NMR Bruker MSL 500 MHz spectrometer. The spectra of the hydrogels were obtained after seasoning and milling to particle sizes ranging from 300 to 425 mm. All measurements were carried out at room temperature.

2.3.3. Thermal analysis

Differential thermal analysis (DTA) and thermogravimetric analysis (TGA) of the hydrogel samples were carried out in a Perkin Elmer instrument in nitrogen atmosphere at the scanning rate of 10 °C/min in the temperature range of 25–600 °C.

2.3.4. X-ray diffraction (XRD)

Wide angle XRD profile of the gel samples was studied at room temperature in a diffractometer (model: X'Pert PRO, made by PANalytical B.V., The Netherlands) using Ni-filtered Cu K_α radiation ($\lambda = 1.5418$ Å) and a scanning rate of 0.005° (2θ/s). The angle of diffraction was varied from 2 to 72°.

2.4. Swelling and deswelling experiments

For studying dynamic swelling properties the xerogel samples were immersed in double distilled water at ambient temperature and mass of the swollen gel sample (m_t) was taken at different time intervals until there was no change of mass with time. The swelling ratio (SR) of the hydrogels was determined by using the following Eq. (3).

$$SR = \frac{m_t - m_d}{m_d} \quad (3)$$

The amount of water absorbed by the different hydrogels under equilibrium conditions, also called equilibrium swelling ratio (ESR) was obtained when mass of the hydrogel (m_e) did not change any more with time. For deswelling, the equilibrated hydrogels were quickly taken out and weighed (m_e) after removing the excess water from its surface with tissue paper. This swollen gel was then weighed at several time intervals (m_{st}) till there is no change in weight. The water retention (WR) was defined as

$$WR = \frac{m_{st}}{m_e} \times 100 \quad (4)$$

2.5. Study of drug loading and entrapment efficiency of the hydrogel

Drug loading and entrapment efficiency of the hydrogel samples were carried out by similar experiments as reported elsewhere (Hua et al., 2010). For drug loading the hydrogel samples of specified weight (m_i) were first swollen in 100 mL water–ethanol mixture (20% ethanol (v/v)) of constant pH and ionic strength (pH 1.5 simulating gastric fluid and 7.5 simulating intestine fluid and ionic strength 0.1 mol/L) and containing specified amount (m_o) of theophylline or tinidazole drug. After 72 h of swelling, the drug loaded wet hydrogel samples were carefully taken out from the solution and washed with the same solution to remove free drug from the sample. Drug loading (DL) and entrapment efficiency of the hydrogel sample was determined as

$$DL\,(mg/g\ hydrogel\ sample) = \frac{m_d - m_i}{m_i} \quad (5)$$

$$Entrapment\ efficiency\,(\%) = \frac{m_d - m_i}{m_o} \times 100 \quad (5a)$$

where m_d is weight of the drug loaded dry hydrogel sample.

2.6. In vitro drug release studies

In vitro release of the drugs from the hydrogel samples was carried out at 35 ± 0.5 °C using Indian Pharmacopoeia (IP) Dissolution Test Apparatus Type 2 (paddle method) at a rotation speed of 50 rpm in 100 mL of buffer (pH 1.5 and 7.5) for 7–9 h. The drug loaded wet samples obtained from drug loading test were first dried overnight at ambient condition followed by drying in a vacuum oven at 50 °C for another three days. The drug loaded dry samples were then immersed in buffer solution of same composition. At several time intervals 5 mL of the solution containing released drug was withdrawn and at the same time 5 mL fresh solution was added to keep the solution volume constant. The concentration of drug in the withdrawn solution was analyzed by UV–vis spectrophotometer (Lamda 25, Perkin Elmer, Singapore) at λ_{max} of 272 nm for theophylline and 310 nm for tinidazole using a calibration curve constructed from a series of the drug solutions of known concentrations. All release experiments were carried out in triplicates and the average values were considered. The drug release % was obtained as

$$Drug\ release\,(\%) = \frac{m_{drug} - m_{release}}{m_{release}} \times 100 \quad (5b)$$

where m_{drug} is mass of drug loaded gel sample and $m_{release}$ is mass of drug released in the solution.

3. Results and discussion

3.1. Synthesis of composite hydrogels

In the present work acrylic acid and MBA undergoes free radical crosslink copolymerization in water in the presence of CS. During free radical polymerization two acrylic monomers copolymerize with two vinyl (—CH=CH—) functional groups of one MBA monomer and thus a three dimensional network of crosslink copolymer gel is formed as shown in the Scheme 1. The initiator also generates free radical on CS present in the polymerization mixture (Panic et al., 2013) and these CS macroradicals take part in the reaction by (i) reacting with another CS radical to form crosslink network and (ii) reacting with radicals of monomers as shown in Scheme 1. Further, some of the ($—NH_2$) groups of CS reacts with carboxylic (—COOH) functional groups of acrylic acid (Lee et al., 1999) to form polyeletrolyte type complex ($NH_3^+COO^-$). Accordingly, a stable composite gel is formed where the dispersed phase, i.e., CS is chemically and ionically bonded to the continuous acrylic phase. The formation of the composite gel is shown in Scheme 1 while the structure of the two drug molecules viz. theophylline and tinidazole is shown in Fig. 1ai and ii, respectively.

3.1.1. Effect of reaction variables on gel content and gel time of the hydrogels

The effect of initiator (I), monomer (AA), crosslinker (MBA) and chitosan (CS) on gel content (%), yield (%) and gel time of the hydrogels are shown in Fig. 1b. For studying effect of one parameter, other parameters were kept constant viz. when concentration of initiator

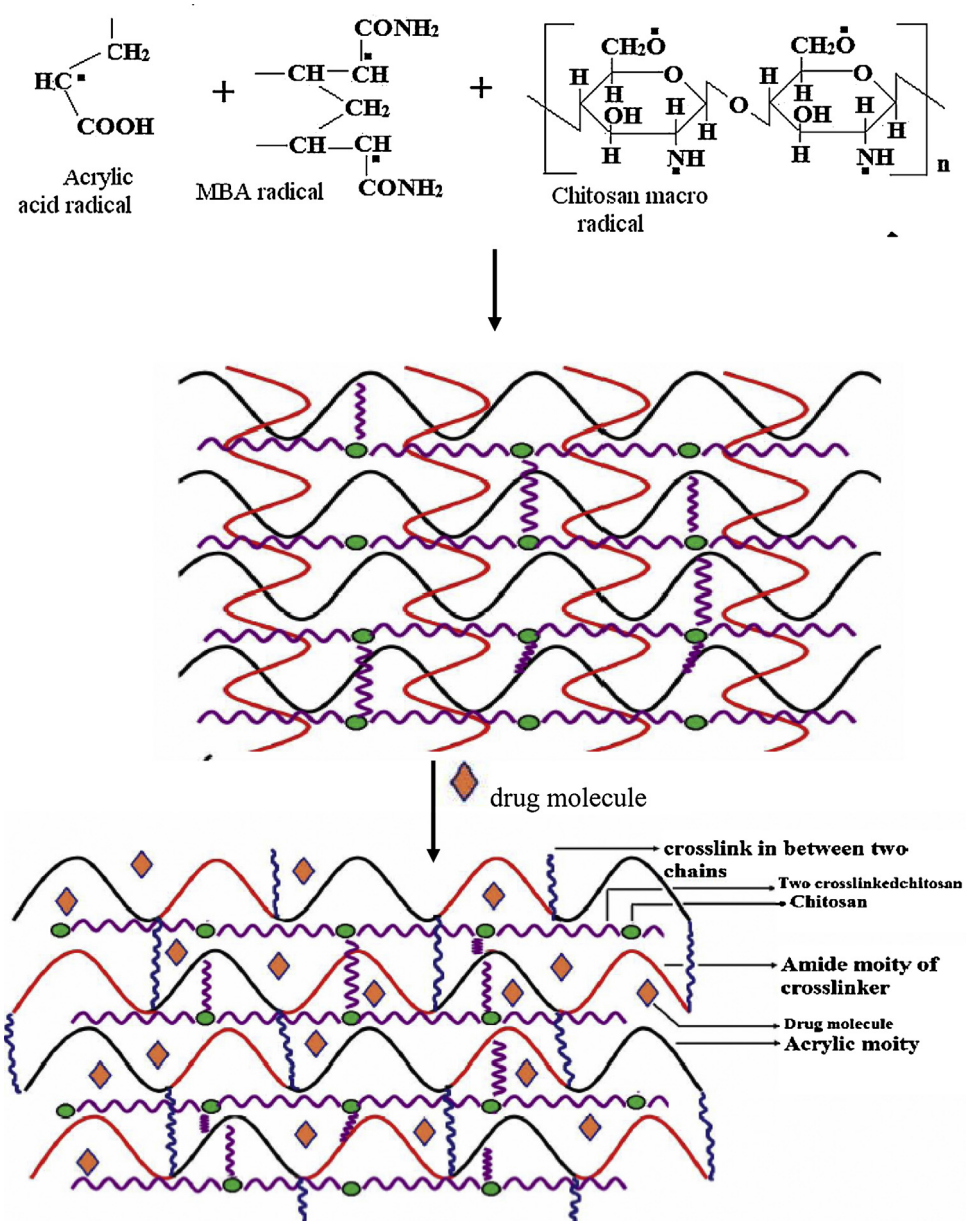

Scheme 1. Formation of composite hydrogel.

was varied as 0.25, 0.5, 0.75 and 1 wt% (of total monomer weight), the amount of crosslinker and monomer were kept constant at 2 wt% and 25 wt%, respectively. From Fig. 1b it is observed that with increase in initiator concentration from 0.5 to 1 wt% yield or gel% and gel time decrease. In fact, rate of polymerization increases at higher initiator concentration resulting in polymer gel of shorter chain length (lower molecular weight). Thus, gelling occurs at an early stage of polymerization resulting in shorter gel time and less gel% (Mall, Srivastava, Kumar, & Mishra, 2006). At very low initiator concentration viz., 0.25 wt% initiator, the initiation of free radicals from initiator is too low. Thus, yield or gel% is observed to increase from 0.25 to 0.5 wt% initiator in polymerization mixtures. From this figure it is observed that with increase in crosslinker concentration gel time decreases. This is because the network (gel) in the polymer is formed at a much faster rate in the presence of increased amount of crosslinker, i.e., MBA. Similarly, yield or gel% also increases with concentration of crosslinker due to increase in rate of polymerization in the presence of increased amount of reactant (crosslinker). However, at 2 wt% crosslinker, yield or gel% decreases because of formation of network at an early stage of polymerization (Bhattacharyya, Ray, & Mandal, 2013). The effect of total monomer concentration in reaction medium on synthesis of gel is also shown in Fig. 1b. With increase in monomer (acrylic acid, AA) concentration in water yield or gel% is observed to increase which may be attributed to generation of large number of active primary radicals at higher monomer concentration in water (Odian, 1991). It is also observed that gel time decreases with increase in monomer concentration in water. This is because gelling occurs early due to increased reaction rate at higher monomer concentration. From Fig. 1b it is also observed that gel time, yield% and gel% increases with increase in wt% of chitosan in the hydrogel. At higher concentration of high molecular weight polymer CS, the solution viscosity increases and the same amount of MBA and acrylic acid take longer time to gel in the viscous medium. However, CS also takes part in the polymerization reaction by forming macro-radicals and hence yields or gel% is observed to increase with increase in amount of

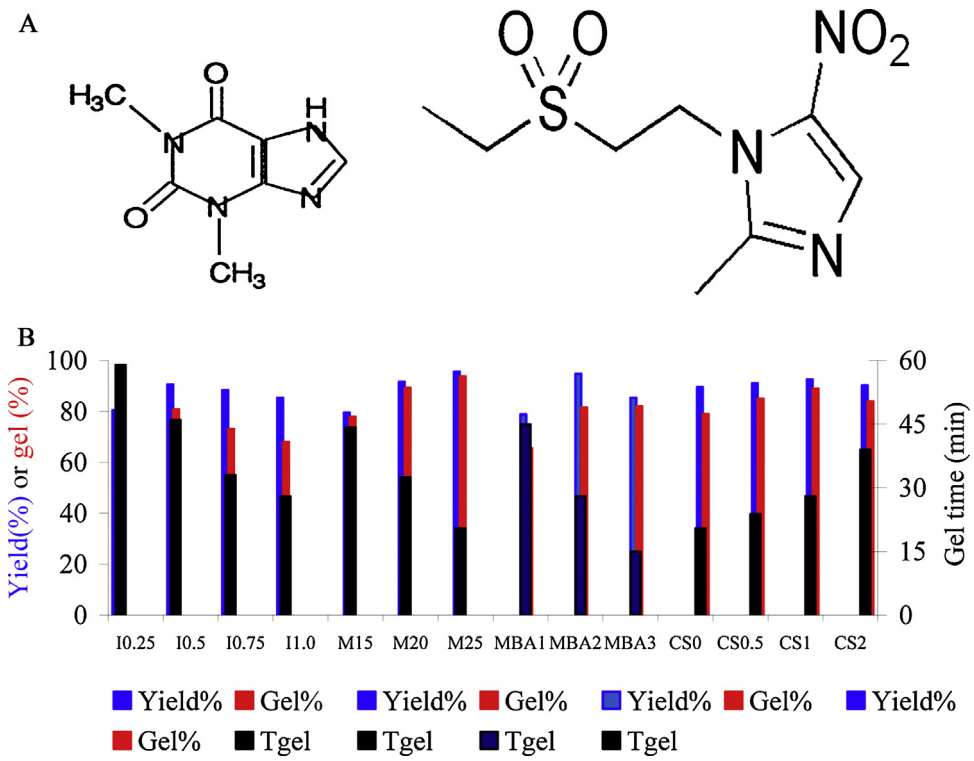

Fig. 1. (a) Structure of drug: (i) theophylline and (ii) tinidazole. (b) Effect of initiator (I), monomer (M), crosslinker (MBA) and chitosan (CS) on yield or gel% and gel time (Tgel).

CS in the hydrogel. At 2 wt% CS viscosities of the reaction medium increases significantly and hence extent of polymerization reaction deceases with decrease in yield or gel%.

3.2. Characterization of the hydrogels

3.2.1. FTIR spectra

The FTIR spectra of the CS, PAACS composite gel, theophylline and tinidazole drugs and drug loaded PAACS gel are shown in Fig. 2a. The pure CS shows characteristic absorption band at 3402 cm^{-1} corresponding to overlapping of its —OH stretching vibration, symmetric N—H vibration and the intermolecular hydrogen bonding of the polysaccharide moiety of CS, 2920 and 2886 cm^{-1} corresponding to C—H stretching vibration (Dai, Yan, Yanga, & Cheng, 2010; Vaghani, Patel, & Satish, 2012). It also shows absorption bands at 1657 cm^{-1}, 1564 cm^{-1} and 1323 cm^{-1} for carbonyl stretching vibration (amide-I), N—H stretching vibration (amide-II) and C—N stretching vibration (amide-III), respectively while absorption at 1379 and 1419 cm^{-1} are due to symmetrical deformation of its methyl (CH_3) groups (Ahmed, Naik, & Sherigara, 2009). From Fig. 2 it is also observed that the —OH stretching of CS is shifted to 3169 cm^{-1} while amide-I, -II and -III stretching of CS is shifted to 1732, 1704 and 1401 cm^{-1}, respectively in PAACS hydrogel. The composite hydrogel also shows a characteristic peak at 1394 cm^{-1} due to symmetric stretching of its caboxylate (COO^-) group while the peak at 1538 cm^{-1} corresponds to its protonated amine (NH_3^+) groups. The carboxylate (COO^-) and protonated amine groups (NH_3^+) are present in the composite hydrogels due to the formation of poly ion complex ($COO^-NH_3^+$) between the amino (NH_3) groups of CS and the carboxylic (COOH) groups of PAA. The FTIR of theophylline shows absorption bands at 3404 and 1567 cm^{-1} for its N—H stretching and bending, respectively, 1723 cm^{-1} for carbonyl (C=O) stretching and 1242 cm^{-1} for C—N vibration (Sullad et al., 2010a, 2010b). Similarly, tinidazole is observed to show absorption bands at 2993 cm^{-1}, 1683 cm^{-1}, 1669 cm^{-1}, 1364 cm^{-1}, 1191 cm^{-1} and 885 cm^{-1}, corresponding to stretching vibration of its C—H, C=C, C—N, N=O, S=O and N—O, respectively (Dash, Ferri, & Chiellini, 2012). The FTIR of theophylline and tinidazole loaded composite gel is also shown in Fig. 3. From these FTIR of drug loaded composite gels no significant change of the major absorption bands of the drugs are observed, i.e., 3404, 1567, 1723, 2916 and 3122 cm^{-1} bands of pure theophylline is observed at 3402, 1567, 1715, 2927 and 3123 cm^{-1} in the theophylline loaded PAA-CS composite gel. Similarly, absorption bands of tinidazole at 2993 cm^{-1}, 1683 cm^{-1}, 1669 cm^{-1}, 1364 cm^{-1}, 1191 cm^{-1} and 885 cm^{-1} is also observed at 2998, 1694, 1667, 1402, 1140 and 884 cm^{-1} in the tinidazole loaded PAA-CS hydrogel. Hence, from the FTIR analysis of the drug free and drug loaded hydrogels it is evident that (i) there exist strong electrostatic interactions between CS and PAA in composite hydrogels of PAA-CS while (ii) there is no significant interaction between the drug molecules and the composite gel.

3.2.2. NMR of the hydrogel

The ^{13}C NMR of the polyacrylic acid and PAACS composite gel are shown in Fig. 2bi and ii. In Fig. 2bi two large peaks are observed at 39.5 and 177.56 ppm corresponding to main carbon–carbon backbone (—CH_2—CHCOOH—) of polymer chain and C atom of carboxylic (COOH) groups, respectively. In the composite hydrogel due to electrostatic interactions between CS and polyacrylic acid, the 39.5 ppm peak of the acid is shifted to 38.98 and 177.56 ppm peak is shifted to 176.19 ppm. Further, the composite gel shows small peaks at 95.92, 71.98 and 58.78 ppm corresponding to C-1, C-3 and C-6 of chitosan (Dorkoosh et al., 2000; Sun, Du, Fan, Chen, & Yang, 2006).

3.2.3. DTA and TGA

The DTA and TGA of the hydrogel samples are shown in Fig. 2ci and ii. From the DTA curves it is observed that uncrosslinked chitosan shows an endothermic peak at around 80 °C corresponding to its glass transition temperature (T_g). However, after incorporation of CS in the gel matrix of crosslink polyacrylic acid this endothermic

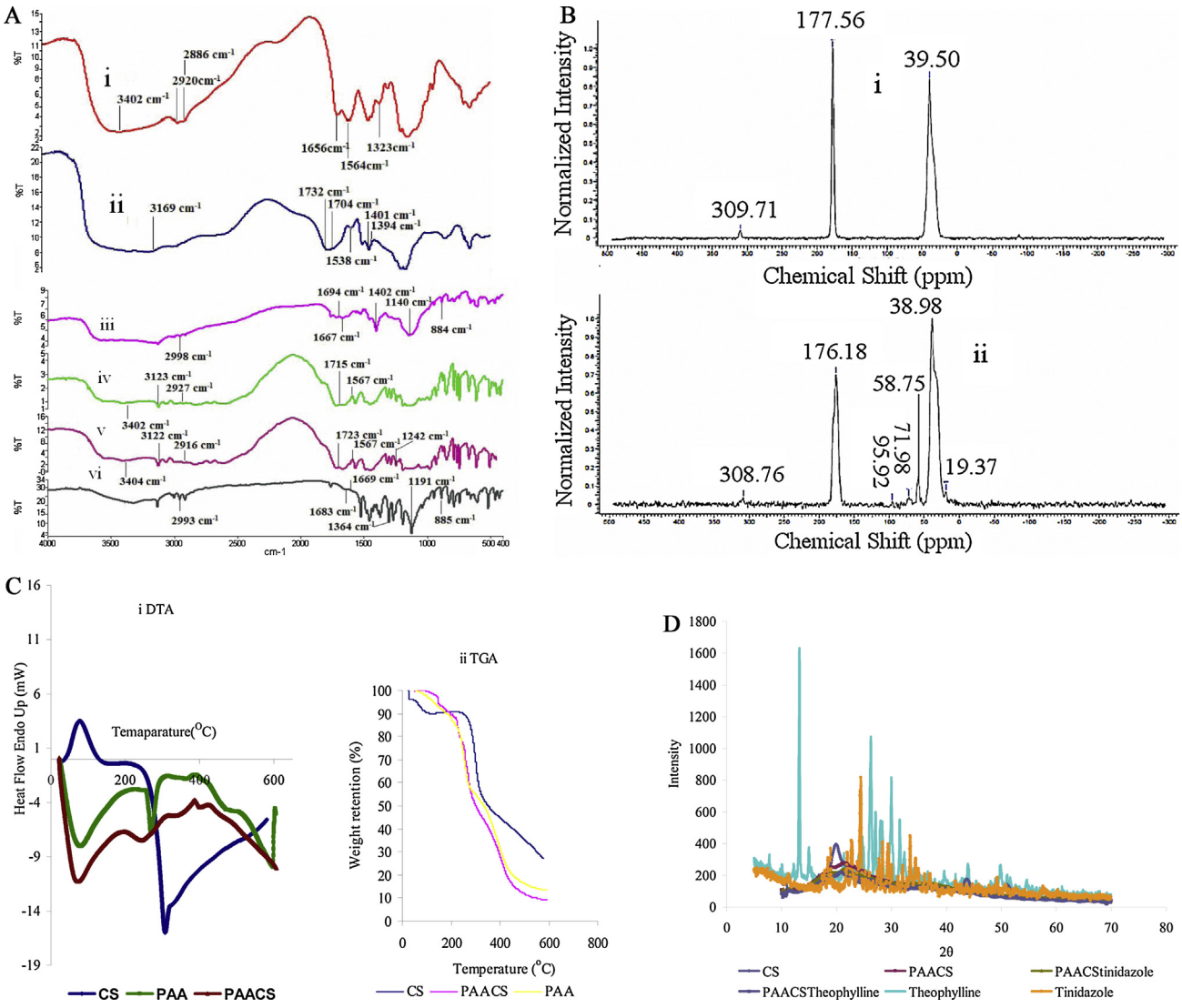

Fig. 2. (a) FTIR of the polymer: (i) CS, (ii) PAACS, (iii) theophylline loaded PAACS (PAACStheophyllene), (iv) PAACS tinidazole, (v) theophylline drug and (vi) tinidazole drug. (b) ^{13}C NMR of (i) polyacrylic acid (PAA) gel and (ii) PAACS composite gel. (c) (i) DTA and (ii) TGA of the polymer. (d) XRD of the polymer and drugs.

peak disappears. In fact, in the crosslinked and network gel the segmental motion of CS chain is restricted. Formation of polyion complex (as evident from FTIR results) between CS and polyacrylic acid further reduces chain mobility of small amount of CS present in the PAA-CS composite gel. Thus, instead of a sharp endothermic peak, the composite gel shows a broadened endothermic peak at around 180 °C. The CS is also observed to show two exothermic peaks at around 309 °C and 325 °C corresponding to thermal decomposition of its amino and N-acetyl residue (Nam, Park, Ihm, & Hudson, 2010) while crosslinked polyacrylic acid shows its exothermic degradation peaks at 270 °C and 473 °C. The composite gel is observed to show degradation at a lower temperature viz. 251 and 403 °C as observed in its DTA in Fig. 4i. TGA of the polymers are shown in Fig. 2cii. From Fig. 2cii it is observed that CS shows around 10 wt% loss in the temperature range of 90–260 °C due to loss of absorbed water. It also show around 15–51% weight loss in the temperature region of 270–360 °C due to degradation of main chain of CS (Rajendran & Sivalingam, 2013) with a residue of about 27% at 580 °C. The first degradation regime corresponds to random splitting of its glycosidic bonds while the second degradation regime (270–360 °C) corresponds to further decomposition and formation of a series of lower fatty acids of C2, C3 and C6 (Milosavljević, ZMilašinović, Popović, Filipović, & Krušić, 2011). From the same figure crosslink polyacrylic acid gel is also observed to show several degradation profiles. Thus, it shows around 10% weight loss in the temperature region of 100–185 °C, 15–30% weight loss in the temperature range of 190–390 °C, 30–75% in the temperature range of 395–490 °C with a residue of around 15% at 580 °C. The first region of degradation corresponds to loss of bound water while the degradations at other temperature regions may be ascribed to splitting of main chain and pendant carboxylic groups of acid (Milosavljević et al., 2011).

3.2.4. X-ray diffraction (XRD)

The XRD of the drug free and drug loaded polymer samples are shown in Fig. 2d. CS being a semi-crystalline polymer shows a strong diffraction peak at 20° associated with mixture of (0 0 1) and (1 0 0) plane and one weak diffraction peak at 10.7° associated with mixture of its (0 0 1) and (1 0 0) planes (Dash et al., 2012; Lee et al., 1999; Qi, Xu, Jiang, Hu, & Zou, 2004). In the PAA-CS composite these XRD peaks of CS is reduced to a great extent along with marginal shifting of 2θ viz. 20° peak of CS is shifted to 21.7° while 10.7° is shifted to 11.9° because of formation of ionic complexes between amine groups of CS and carboxylic groups of polyacrylic

acid. The drug theophylline being crystalline shows several XRD peaks at 2θ of 13.2°, 14.9°, 24°, 26.2° and 30° (Lin, Huang, Chang, & Jiahui, 2011) while tinidazole is observed to show major XRD peaks at 18.9°, 22.7°, 24.4°, 28.4°, 29.4°, 33.3° and 49.3°. Most of these peaks of the two drugs disappear and some of these show shifting of these 2θ values with much reduction in peak intensity. The drugs after dissolution in water loss its crystallinity and aqueous solution of the amorphous drug is absorbed by the hydrogels. After drying within the gel, however, the drug cannot crystallize within the restricted network of the gel matrix which results in loss of its XRD peaks.

3.3. Study of swelling of the hydrogels

Several hydrogels synthesized by varying concentration of monomer (acrylic acid), initiator, crosslinker (MBA) and CS were used for swelling at different time intervals in double distilled water. The results of swelling viz. equilibrium swelling ratio (ESR) and equilibrium swelling time (t_{eq}) in water for all of these hydrogels are shown in Fig. 3a. From this figure it is observed that both ESR and t_{eq} decreases with increase in initiator concentration. At higher initiator concentration hydrogels of low molecular weight with more chain ends are formed resulting in low ESR and low t_{eq} because of network imperfection in the gel (Chang, Duan, Cai, & Zhang, 2010; Jeon, Lei, & Kim, 2008). Similarly, increase in crosslinker concentration results in tighter and denser network of the gel. Consequently, ESR decreases at higher crosslinker concentration while t_{eq} increases since water molecules take longer time to fill a dense network to reach swelling equilibrium. Similarly, with increase in total monomer concentration, ESR increases while t_{eq} decreases. Based on the swelling results as shown in Fig. 3a, the hydrogel synthesized with 25 wt% monomer, 0.5 wt% initiator and 2 wt% crosslinker was chosen and further filled with 0.5, 1, and 2 wt% chitosan (CS). The ESR is observed to increase further when the polyacrylic acid gel (PAA) is filled with CS. However, above 1 wt% CS, the ESR of the composite gel decreases. The CS contains both —OH and —NH_2 groups and thus in the presence of CS ESR increases. However, CS also fills up the network of the gel and above 1 wt% CS, there is a marginal decrease in ESR as observed in Fig. 3a. In the PAACS composite gel the filled network takes longer time for penetration of water and hence t_{eq} increases with increase in CS content. The hydrogel containing 1 wt% CS and showing the highest ESR was also subjected to swelling at varied pH and this hydrogel is observed to show ESR of 10.3, 18.1 and 25.2 at pH of 1.5, 6.5 and 7.6, respectively. The swelling at low pH is due to the protonation of the amino groups of the CS present in the hydrogel. As the amino groups are protonated, they are ionized. This ionization causes swelling due to electrostatic repulsion. The amino groups of CS remain protonated up to its point of zero charge pH which is 9.9 (Wang et al., 2008). Similarly, the carboxylic groups (COOH) of the gel ionize at a pH above its pK_a value (4.26). Thus, ESR increases further at higher pH. Similarly, from Fig. 3a it is also observed that the pH responsive composite gel shows varied ESR when ionic strength of the solution is increased viz. ESR decreases with increase in molar concentration of salt from 0.05 molar to 0.2 molar in the presence of monovalent sodium chloride, bivalent calcium chloride or trivalent aluminium chloride. Similarly, for the same molar concentration of the solution, ESR is observed to decrease from monovalent sodium chloride to trivalent aluminium chloride salt. The ionic strength of the solution increases with increase in molar concentration or from monovalent to trivalent salt. Consequently the electric double layers surrounding the functional groups of the gels compress resulting in decrease in ESR.

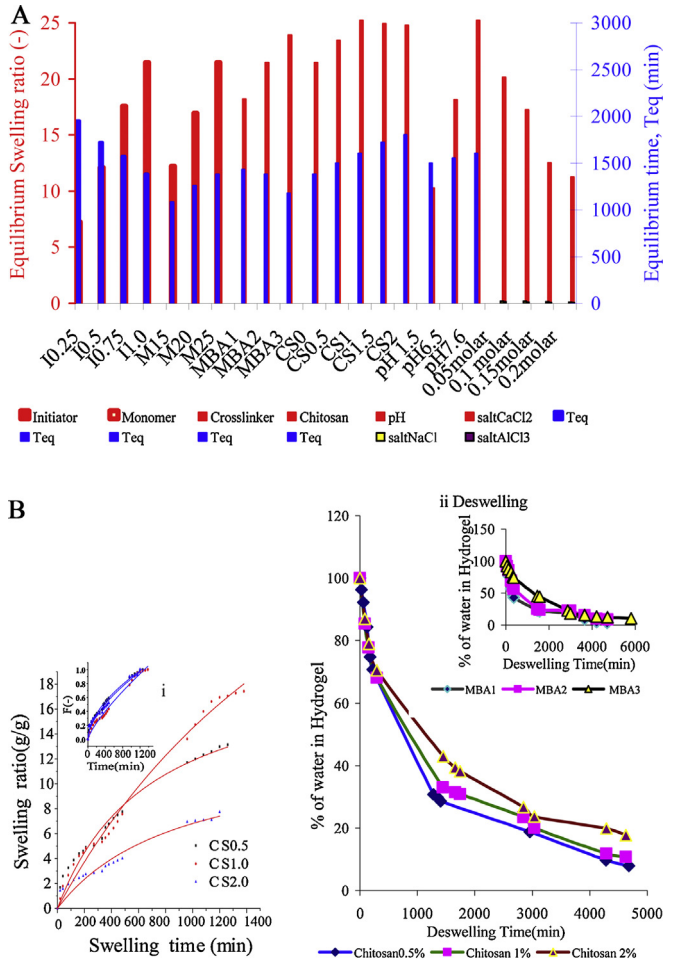

Fig. 3. (a) Effect of conc. of initiator, total monomer, crosslinker, chitosan, salt and pH on equilibrium swelling ratio. (b) (i) Non-linear fitting of swelling data to 2nd order rate equation and diffusion characteristics (inset) at varied CS wt%, (ii) deswelling of the hydrogel at varied CS wt% and crosslinker (MBA) wt% (inset).

3.3.1. Swelling kinetics, diffusion and network parameters

3.3.1.1. Swelling kinetics. The swelling ratio (SR) of the hydrogels at various time intervals was observed to fit well to the following non-linear second order rate Eq. (6) (Mall et al., 2006)

$$SR_t = \frac{m_e^2 k_{S2} t}{1 + k_{S2} m_e t} = \frac{r_o t}{1 + k_{S2} m_e t} \quad (6)$$

here, k_{s2} is rate constant and r_o is initial rate of swelling.

The data fitting were carried out by using Levenberg–Marquardt (L–M) algorithm (Origin-8 software) with adjustment of parameter values viz. rate constant (k_{s2}) and initial rate of swelling (r_0) by iteration using chi square (χ^2) and F values (Samanta & Ray, 2014). The trend lines of these non-linear fittings for hydrogels synthesized with 0.5, 1 and 2 wt% CS and designated as CS0.5, CS1.0 and CS2.0, respectively, are shown in Fig. 3bi. Similar trend lines (not shown) were also obtained for hydrogels synthesized with 1, 2 and 3 wt% crosslinker (designated as MBA1, MBA2 and MBA3, respectively), 15, 20 and 25 wt% acrylic acid (monomer) in water (designated as AA15, AA20 and AA25, respectively). The values of k_{s2} and r_0, experimental and calculated ESR of all of these hydrogels are shown in Table 1. The values of statistical parameters, i.e., r^2, χ^2 and F are also shown in Table 1. It is observed that ESR of the hydrogels calculated using second order rate Eq. (6) closely matches the experimental ESR. The values of regression coefficients (r^2) for all of these fittings are also observed to be close to unity while these regressions also show low χ^2 and high F values. All of these results confirm good fitting of the swelling data to second order rate equation.

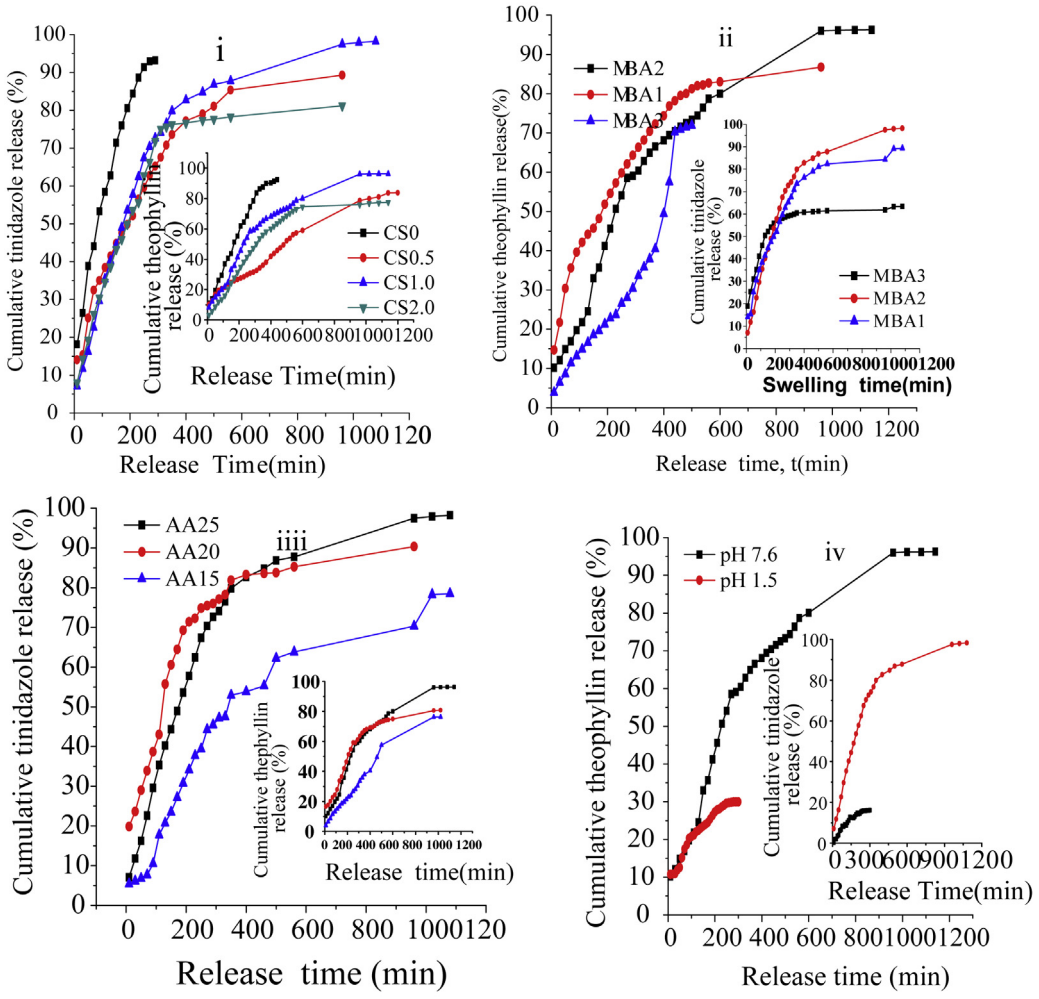

Fig. 4. Cumulative release% of theophylline and tinidazole drug at (i) varied CS wt%, (ii) MBA wt%, (iii) monomer (acrylic acid) wt% and (iv) pH for CS1.0 gel.

3.3.1.2. Diffusion. The study of diffusion through network of hydrogel is pertinent for its application in drug release. The diffusion in polymer is passive but it can be activated by swelling in release medium, i.e., water in the present case and also by various external physical forces like polar, osmotic or convective forces (Akdemir & Apohan, 2007). For understanding the diffusion mechanism, the swelling data were also fitted to the following Eqs. (7) and (8) (Ritger & Peppas, 1987) to obtain the diffusion characteristics viz. diffusion constant (k_D), diffusional exponent (n) and diffusion coefficient (D) of the hydrogels.

$$F = \frac{m_t}{m_e} = k_D t^n \tag{7}$$

$$D = \pi r^2 \left(\frac{k_D}{4}\right)^{1/n} \tag{8}$$

Table 1
Swelling diffusion and network parameters of the hydrogels.

Polymer	k_{s2}/r_0	ESR_{expt}/ESR_{cal} (g/g)	$r^2/\chi^2/F$	$k_D/n/D \times 10^5$	$r^2/\chi^2/F$	$M_c \times 10^{-6}/\rho_c \times 10^{-17}/\varsigma$
MBA1	0.001931/0.0323	13.06/14.84	0.96/0.0.449/910	0.018/0.57/2.5	0.963/0.0008/3363	21/0.53/916
MBA2	0.0022/0.019	8.39/8.911	0.993/0.294/1365	0.041/0.39/1.81	0.990/0.0011/1920	3.3/4.14/812
MBA3	0.009101/0.0705	6.32/5.46	0.937/0.169/1238	0.143/0.27/4.58	0.987/0.0009/5882	7.46/3.52/416
I1.0	0.0025/0.0174	7.073/8.190	0.996/0.063/1885	0.038/0.42/3.32	0.951/0.0018/474	3.1/10.81/341
I0.75	0.0023/0.028	11.3/12.56	0.986/0.610/280	0.043/0.38/2.23	0.998/0.0013/1779	3.2/5.52/417
I0.5	0.0022/0.019	8.39/8.911	0.993/0.294/1365	0.041/0.39/1.81	0.990/0.0011/1920	3.3/4.14/812
I0.25	0.0048/0.038	7.252/7.87	0.953/0.038/3029	0.148/0.28/1.84	0.9675/0.002/379	3.73/2.7/1261
CS0.5	0.001790/0.029	13.157/14.47	0.992/0.132/4906	0.018/0.56/3.50	0.995/0.0014/5398	3.78/2.1/846
CS1.0	0.001398/0.0295	16.32/19.74	0.996/0.306/3723	0.011/0.63/4.53	0.998/0.0042/1979	6.2/1.62/854
CS2.0	0.001013/0.013	7.18/8.94	0.972/0.12/1423	0.012/0.62/1.18	0.908/0.0036/1746	1.38/2.4/421
AA15	0.0020/0.0382	6.112/7.765	0.952/0.21/406	0.023/0.53/5.6	0.955/0.013/108	6.23/1.62/378
AA20	0.0013/0.0201	7.433/8.16	0.986/0.80/423	0.013/0.63/7.91	0.988/0.002/829	10/0.8/817
AA25	0.0022/0.019	8.39/8.911	0.993/0.294/1365	0.041/0.39/1.81	0.990/0.0011/1920	3.3/4.14/812

k_{s2} (g gel/g water min), r_0 (g water/g gel min), k_D, n, D (cm^2/s).

where F is fractional water uptake and r is radius of cylindrical hydrogel sample. The data fitting and non-linear regression was similar to swelling kinetics as shown in inset of Fig. 3bi for CS0.5, CS1.0 and CS2.0 composite gels. Similar trendlines were obtained for other hydrogels. The values of diffusion characteristics, i.e., k_D, n and D of the hydrogels are also shown in Table 1. From Table 1 it is observed that hydrogels prepared with varied CS, MBA and acrylic acid concentration shows n values ranging from 0.5 to around 0.7 signifying Non-Fickian anamolous diffusion, i.e., in these cases rate of diffusion and rate of chain relaxation of the gels are comparable. The hydrogels prepared with varied initiator concentrations shows n values close to 0.5 indicating Fickian Case-1 diffusion, i.e., in these cases rate of diffusion is slightly lower than rate of chain relaxation (Tomić, Mićić, Filipović, & Suljovrujic, 2007). The values of statistical parameters, i.e., r^2, χ^2 and F for these non-linear fittings as shown in Table 1 also confirms good fitting of swelling data to diffusion equation.

3.3.1.3. Network parameters. The network structure of the hydrogels was characterized in terms of network parameters, i.e., average molecular weight between crosslink (M_c), crosslink density (ρ_c) and mesh size (ς). These parameters were determined from swelling data based on network theory of Flory and Rehner as reported elsewhere (Bhattacharyya et al., 2013; Samanta & Ray, 2014). The value of M_c, ρ_c and ς of the hydrogels are also given in Table 1. In general, the small M_c and ς value and high ρ_c value signifies tighter network. From Table 1 it is observed that that with increase in crosslinker (MBA) concentration M_c and ς decreases while ρ_c increases, i.e., increase in crosslinker concentration results in tighter network. Similarly, with decrease in initiator concentration from I1.0 to I0.25, molecular weight of the polymer increases (Odian, 1991) and hence both M_c and ς increases while ρ_c decreases. From Table 1 it is also observed that with increase in wt% of CS in the gel from CS0.5 to CS1.0, M_c and ς of the hydrogel increases which may be due to formation of multiple branched structures (Wang & Wang, 2010) in the gel. However, as the wt% of CS is increased further to 1 wt%, M_c and ς decreases. In fact, above 1 wt% CS, the solution viscosity increases to a great extent. Consequently initiation efficiency of CS decreases and its effect on network parameter also reduces (Wang & Wang, 2010). Similar trend of network parameters are observed in Table 1 for hydrogels synthesized with varied monomer (acrylic acid) concentration, i.e., for AA15, AA20 and AA25 gels.

3.3.2. Deswelling kinetics of the hydrogels

The response rate of a drug loaded hydrogel may be evaluated in terms of deswelling of the water swollen hydrogels. The results of deswelling of the hydrogels with varied crosslinker and CS wt% at 25 °C is shown in Fig. 3bii. In general for any hydrogel, deswelling rate is much faster than swelling rate. This is because of formation of a dense skin layer on the surface of the hydrogel in contact with water by rapid shrinkage due to electrostatic interaction among various hydrophobic groups on its surface. Consequently, water cannot diffuse out easily from this dense layer (Marandi, Sharifnia, & Hosseinzadeh, 2006; Samanta & Ray, 2014). However, incorporation of hydrophilic CS retards formation of this preventive skin layer and act as a water releasing channel in the composite gel structure (Marandi et al., 2006). Thus, rate of deswelling is observed to increase with increase in wt% of CS from CS0.5 to CS2.0. From this Fig. 3bii it is also observed that deswelling rate decreases with increase in % of crosslinker which may be attributed to the formation of tighter network at higher crosslinker%.

Table 2
Drug release data of the hydrogels.

Polymer	THEO/TNZ loading (mg/100 mg beads)	Entrapment efficiency (%)
CS0	19.11/17.56	50.75/48.37
CS0.5	22.11/20.04	68.30/64.12
CS1.0	28.91/26.51	77.42/70.45
CS2.0	29/26.5	81.58/79.56
MBA1	27.21/25.76	63.77/61.22
MBA2	19.11/17.56	50.75/48.37
MBA3	14.21/13.93	43.58/41.56
AA15	13.24/12.67	72.55/68.12
AA20	15.23/14.11	44.34/41.34
AA25	19.11/17.56	50.75/48.37
CS1 at pH 1.5	16.23/14.72	44.2/41.6
CS1 at pH 7.5	28.91/26.51	77.42/70.45

3.4. In vitro drug release study

The loading and entrapment efficiency of theophylline and tinidazole drug for various hydrogels are shown in Table 2. Similar to swelling ratio, loading and entrapment efficiency of these drugs are also observed to increase with decrease in crosslinker wt%, increase in wt% of CS and increase in solution pH from 1.6 to 7.5. The loading or entrapment efficiency of theophylline is observed to be slightly higher than loading or entrapment of tinidazole. From the FTIR results it is evident that there is no significant electrostatic interaction between hydrogel and drug molecules. However, theophyllene appear to be structurally more compact (two fused rings) than tinidazole which may cause its easier incorporation in the gel. The cumulative release profile of these two drugs from these hydrogels is presented in Fig. 4i and ii for varied crosslinker % and CS wt%, respectively. The release profile of CS1.0 hydrogel at pH 7.6 and 1.5 is shown in Fig. 4iii. From all of these figures it is observed that an initial burst release of the drug is followed by a sustained rate of release for all of these hydrogels. Initially the fast release rate of drug occurs from the surface of the hydrogel due to high concentration gradient of the drug between the release medium, i.e., water and the surface of the gel (Patil, Dordick, & Rethwisch, 1996). As the release of the drug continues, its concentration in the release medium increases and hence the concentration gradient of drug between gel and release medium decreases and entrapment of the remaining drug in the gel network slow down further release at low concentration gradient (Zhang, Wu, & Chu, 2004). It is also observed that theophylline shows slightly lower release% than tinidazole. Similar release profiles were reported for release of model protein and drug from various IPN type hydrogels (Kulkarni, Sreedhar, Mutalik, Setty, Sa, 2010; Matricardi et al., 2013; Patil et al., 1996; Raghavendra, Rashmi, Mohan, Mutalik, & Kalyane, 2012; Samanta & Ray, 2014).

3.4.1. Fitting of drug release data to model equations

For evaluating the release kinetics, the first 60% of the drug release data of the hydrogels were fitted to the following (i) Donbrow–Samuelov (Donbrow & Samuelov, 1980) zero-order kinetics (Eq. (9)), (ii) Higuchi model (Higuchi, 1963) (Eq. (10)), and (iii) Korsmeyer–Peppas model (Korsmeyer, Gurny, Doelker, Buri, & Peppas, 1983) (Eq. (11)). Similar to swelling kinetics non-linear Levenberg–Marquardt (L–M) algorithm (Origin-8 software) was also used for these fittings.

(i) Zero order Donbrow–Samuelov model

$$m_{Dt} = m_{De} + K_0 t \quad (9)$$

(ii) Higuchi model

$$m_{Dt} = m_{De} + K_H t^{1/2} \quad (10)$$

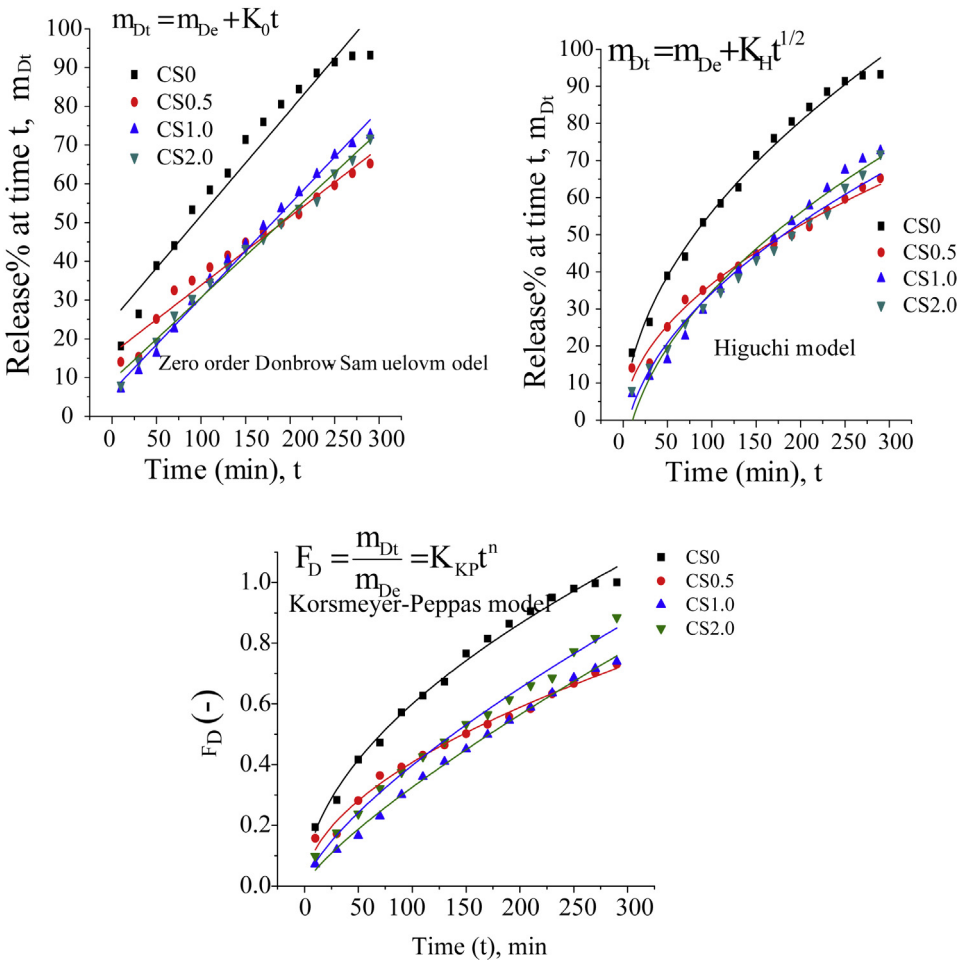

Fig. 5. Fitting of drug release data of tinidazole to (i) Donbrow–Samuelov zero-order, (ii) Higuchi and (iii) Korsmeyer–Peppas model for CS0, CS0.5, CS1.0 and CS2.0 hydrogels.

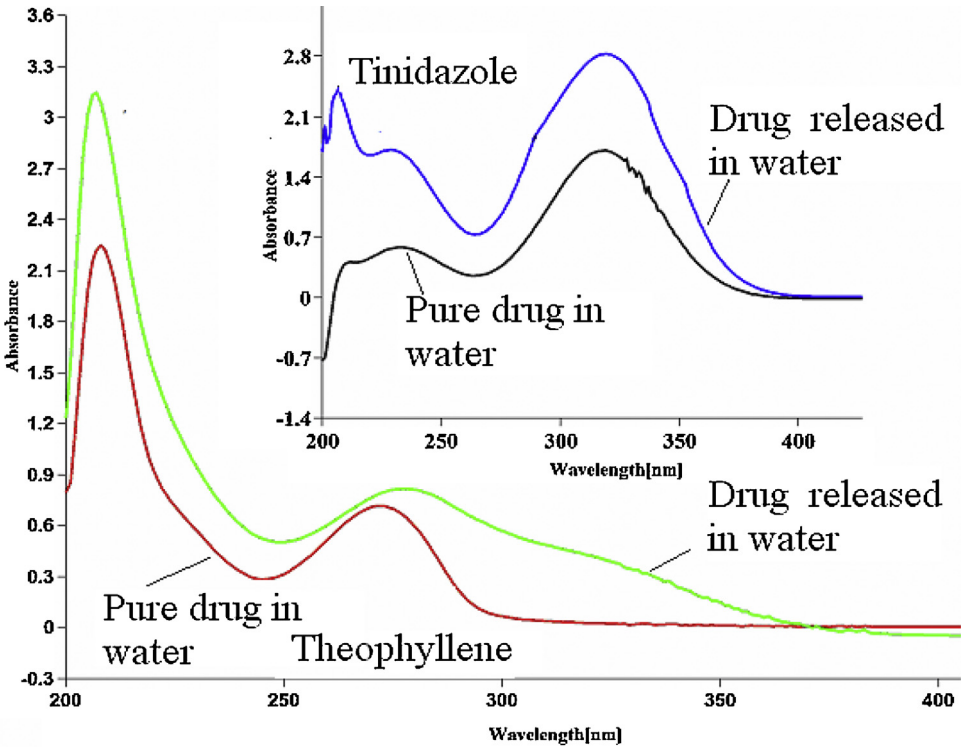

Fig. 6. UV spectra of pure and released drugs in water.

(iii) Korsmeyer–Peppas model

$$F_D = \frac{m_{Dt}}{m_{De}} = K_{KP} t^n \quad (11)$$

where m_{Dt} and m_{De} are amount of drug released at time t and infinity (at equilibrium), respectively, K_0, K_H and K_{KP} are constant of the concerned model corresponding to structural and geometrical character of the dosage form and the diffusion exponent 'n' signifies mechanism of drug release. The fitting of drug release data to these models are shown in Fig. 5i–iii for Donbrow–Samuelov zero order, Higuchi and Korsmeyer–Peppas models, respectively with CS0, CS0.5, CS1.0 and CS2.0 hydrogels. The calculated m_{De} values for zero order fittings were 24.7%, 16.1%, 6.39% and 9.19% corresponding to experimental 18.2, 14.06, 7.1 and 8.02%, i.e., except CS0 other hydrogels show close fitting to this zero order model. The statistical parameters such as r^2 was close to unity (0.951, 0.968, 0.991, 0.992) while χ^2 values were low (22, 8, 3, 3.1) for these fittings (Fig. 5i) which also confirms close fitting except for CS0 hydrogel. Though the statistical parameters are within acceptable range for fitting to Highuchi model (Fig. 5ii) but the data yields negative intercept (m_{De}). However, the drug release data is observed to give close fitting to Korsmeyer–Peppas model. It yields n value of 0.5, 0.53, 0.79 and 0.71 and K_{KP} are observed to be 0.05, 0.35, 0.008 and 0.014 for CS0, CS0.5, CS1.0 and CS2.0 hydrogels, respectively. The values of n indicate diffusion controlled release of drug. These fittings also shows r^2 values close to unity (0.991, 0.987, 0.997 and 0.994) and very low χ^2 value (0.0005, 0.0004, 0.0001 and 0.0003) indicating very close fitting as also observed in Fig. 5iii.

3.4.2. Drug activity

The chemical activity of the drug was investigated by recording the UV spectra of pure theophylline and tinidazole in water and also these drugs released in water from hydrogels at wavelength of 272 nm for theophylline and 310 nm for tinidazole as shown in Fig. 6. The spectra appear to be almost identical suggesting that there was no significant change in chemical and bioactivity of the drug during its loading and release. Similar type of comparison to assess the chemical and bioactivity of drug has also been reported elsewhere (Chouhan & Bajpai, 2010).

4. Conclusion

Composite hydrogels were synthesized by in situ incorporation of chitosan (CS) in polymerization mixtures of acrylic acid and MBA. Several hydrogels were prepared by varying concentration of initiator, weight% of crosslinker (MBA), acrylic acid monomer and CS. These hydrogels were characterized by FTIR, NMR, DTA–TGA and XRD. Swelling data of the hydrogels showed close non-linear fitting to second order rate equation. Diffusional characteristics, molecular weight between two crosslinks, crosslink density and mesh size of the hydrogels were also evaluated. Release profile of theophylline and tinidazole drug from these hydrogels was found to show close fitting to Korsmeyer–Peppas model. The hydrogel synthesized with 1 wt% CS, 0.5 wt% initiator, 2 wt% MBA and 25 wt% acrylic acid in water was observed to show optimum swelling as well as drug entrapment and drug release profile at pH of 7.5.

Acknowledgements

The first author is grateful to TEQUIP Phase-II for providing fellowships. Authors are also grateful to Council of Scientific and Industrial Research (CSIR) and Department of Science and Technology (DST), Govt. of India for their financial support to purchase UV–vis spectrophotometer and FTIR spectrophotometer used for the present work.

References

Ahmed, A. A., Naik, H. S. B., & Sherigara, B. S. (2009). Synthesis and characterization of chitosan-based pH-sensitive semi-interpenetrating network microspheres for controlled release of diclofenac sodium. *Carbohydrate Research*, *344*, 699–706.

Ahn, J. S., Choi, H. K., & Cho, C. S. (2001). A novel mucoadhesive polymer prepared by template polymerization of acrylic acid in the presence of chitosan. *Biomaterials*, *22*, 923–928.

Akdemir, Z. S., & Apohan, N. K. (2007). Investigation of swelling, drug release and diffusion behaviors of poly(N-isopropylacrylamide)/poly(N-vinylpyrrolidone) full-IPN hydrogels. *Polymers for Advanced Technology*, *18*, 932–939.

Bertza, A., Bruhnb, S. W., Sebastian, M., Tierschd, B., Koetzd, J., Hustc, M., et al. (2013). Encapsulation of proteins in hydrogel carrier systems for controlled drug delivery: Influence of network structure and drug size on release rate. *Journal of Biotechnology*, *163*, 243–249.

Bhattacharya, A., Rawlins, J. W., & Ray, P. (2009). *Polymer grafting and crosslinking*. Hoboken, NJ: John Wiley & Sons, Inc.

Bhattacharyya, R., Ray, S. K., & Mandal, B. (2013). A systematic method of synthesizing composite superabsorbent hydrogels from crosslink copolymer for removal of textile dyes from water. *Journal of Industrial and Engineering Chemistry*, *19*, 1191–1203.

Chang, C., Duan, B., Cai, J., & Zhang, L. (2010). Superabsorbent hydrogels based on cellulose for smart swelling and controllable delivery. *European Polymer Journal*, *46*, 92–100.

Chouhan, R., & Bajpai, A. K. (2010). Release dynamics of ciprofloxacin from swellable nanocarriers of poly(2-hydroxyethyl methacrylate): An in vitro study. *Nanomedicine: Nanotechnology, Biology & Medicine*, *6*, 453–462.

Dai, J., Yan, H., Yanga, H., & Cheng, R. (2010). Simple method for preparation of chitosan/poly(acrylic acid) blending hydrogel beads and adsorption of copper(II) from aqueous solutions. *Chemical Engineering Journal*, *165*, 240–249.

Dash, M., Ferri, M., & Chiellini, F. (2012). Synthesis and characterization of semi-interpenetrating polymer network hydrogel based on chitosan and poly(methacryloylglycylglycine). *Materials Chemistry & Physics*, *135*, 1070–1076.

Donbrow, M., & Samuelov, Y. (1980). Zero order drug delivery from double-layered porous films: Release rate profiles from ethyl cellulose, hydroxypropylcellulose and polyethylene glycol mixtures. *Journal of Pharmacy and Pharmacology*, *32*, 463–470.

Dorkoosh, F. A., Brussee, J., Verhoef, J. C., Borchard, G., Rafie-Tehrani, M., & Junginger, H. E. (2000). Preparation and NMR characterization of superporous hydrogels (SPH) and SPH composites. *Polymer*, *41*, 8213–8220.

Higuchi, T. (1963). Mechanism of sustained action medication, theoretical analysis of rate of release of solid drugs dispersed in solid matrices. *International Journal of Pharmaceutics*, *52*, 1145–1149.

Hua, S., Ma, H., Li, X., Yang, H., Wang, A., Hua, S., et al. (2010). pH-sensitive sodium alginate/poly(vinyl alcohol) hydrogel beads prepared by combined Ca^{2+} crosslinking and freeze-thawing cycles for controlled release of diclofenac sodium. *International Journal of Biologica Macromolecules*, *46*, 517–523.

Islam, A., & Yasin, T. (2012). Controlled delivery of drug from pH sensitive chitosan/poly(vinyl alcohol) blend. *Carbohydrate Polymers*, *88*, 1055–1060.

Jameela, S. R., Lakshmi, S., James, N. R., & Jayakrishnan, A. (2002). Preparation and evaluation of photocrosslinkable chitosan as a drug delivery matrix. *Journal of Applied Polymer Science*, *86*, 1873–1877.

Jeon, Y. S., Lei, J., & Kim, J. H. (2008). Dye adsorption characteristics of alginate/polyaspartate hydrogels. *Journal of Industrial and Engineering Chemistry*, *14*, 726–731.

Kajjari, P. B., Manjeshwar, L. S., & Aminabhavi, T. M. (2011). Semi-interpenetrating polymer network hydrogel blend microspheres of gelatin and hydroxyethyl cellulose for controlled release of theophylline. *Industrial & Engineering Chemistry Research*, *50*(13), 7833–7840.

Korsmeyer, R. W., Gurny, R., Doelker, E. M., Buri, P., & Peppas, N. A. (1983). Mechanism of solute release from porous hydrophilic polymers. *International Journal of Pharmaceutics*, *15*, 25–35.

Krishnaiah, Y. S., Bhaskarreddy, P. R., Satyanarayana, S., & Karthikeyan, R. S. (2002). Studies on the development of oral colon targeted drug delivery systems for Tinidazole in the treatment of amoebiasis. *International Journal of Pharmaceutics*, *236*, 43–55.

Kulkarni, R. V., Sreedhar, V., Mutalik, S., Setty, C. M., & Sa, B. (2010). Interpenetrating network hydrogel membranes of sodium alginate and poly(vinyl alcohol) for controlled release of prazosin hydrochloride through skin. *International Journal of Biological Macromolecules*, *47*, 520–527.

Lee, J. W., Kim, S. Y., Kim, S. S., Lee, Y. M., Lee, K. H. Y., & Kim, S. J. (1999). Synthesis and characteristics of interpenetrating polymer network hydrogel composed of chitosan and poly(acrylic acid). *Journal of Applied Polymer Science*, *73*, 113–120.

Lin, N., Huang, J., Chang, P. R., & Jiahui, L. F. (2011). Effect of polysaccharide nanocrystals on structure, properties, and drug release kinetics of alginate-based microspheres. *Colloids and Surfaces B: Biointerfaces*, *85*, 270–279.

Lorenzo, C. A., Fernandez, B. B., Puga, A. M., & Concheiro, A. (2013). Crosslinked ionic polysaccharides for stimuli-sensitive drug delivery. *Advanced Drug Delivery Reviews*, http://dx.doi.org/10.1016/j.addr.2013.04.016

Mall, I. D., Srivastava, V. C., Kumar, G. V. A., & Mishra, I. M. (2006). Characterization and utilization of mesoporous fertilizer plant waste carbon for adsorptive removal of dyes from aqueous solution. *Colloids and Surfaces A: Physicochemical and Engineering Aspects*, *278*, 175–187.

Marandi, G. B., Sharifnia, N., & Hosseinzadeh, H. (2006). Synthesis of an alginate–poly(sodium acrylate-*co*acrylamide) superabsorbent hydrogel with low salt sensitivity and high pH sensitivity. *Journal of Applied Polymer Science*, *101*, 2927–2937.

Mastiholimath, V. S., Dandagi, P. M., Jain, S. S., Gadad, A. P., & Kulkarni, A. R. (2007). Time and pH dependent colon specific, pulsatile delivery of theophylline for nocturnal asthma. *International Journal of Pharmaceutics*, *328*, 49–56.

Matricardi, P., Meo, C. D., Coviello, T., Hennink, W. E., & Alhaique, F. (2013). Interpenetrating polymer networks polysaccharide hydrogels for drug delivery and tissue engineering. *Advanced Drug Delivery Reviews*, http://dx.doi.org/10.1016/j.addr.2013.04.002

Milosavljević, N. B., Milašinović, Z. N., Popović, I. G., Filipović, J. M., & Krušić, M. T. K. (2011). Preparation and characterization of pH-sensitive hydrogels based on chitosan, itaconic acid and methacrylic acid. *Polymer International*, *60*, 443–452.

Nam, Y. S., Park, W. H., Ihm, D., & Hudson, S. M. (2010). Effect of the degree of deacetylation on the thermal decomposition of chitin and chitosan nanofibers. *Carbohydrate Polymers*, *80*, 291–295.

Odian, G. (1991). Radical chain polymerization. In *Principle of polymerization* (Third ed., pp. 198–334). Singapore: John Wiley & Sons Inc.

Paloma, M., Torrea, d., Enobakharea, L., Torradob, Y., & Torrado, G. S. (2003). Release of amoxicillin from polyionic complexes of chitosan and poly(acrylic acid). Study of polymer/polymer and polymer/drug interactions within the network structure. *Biomaterials*, *24*, 1499–1506.

Panic, V. V., Madzarevic, Z. P., Husovic, T. V., & Velickovic, S. J. (2013). Poly(methacrylic acid) based hydrogels as sorbents for removal of cationic dye basic yellow 28: Kinetics, equilibrium study and image analysis. *Chemical Engineering Journal*, *217*, 192–204.

Patil, N. S., Dordick, J. S., & Rethwisch, D. G. (1996). Macroporous poly(sucrose acrylate) hydrogel for controlled release of macromolecules. *Biomaterials*, *17*, 2343–2350.

Qi, L., Xu, Z., Jiang, X., Hu, C., & Zou, X. (2004). Preparation and antibacterial activity of chitosan nanoparticles. *Carbohydrate Research*, *339*, 2693–2700.

Raghavendra, V. K., Rashmi, B., Mohan, G. K., Mutalik, S., & Kalyane, N. V. (2012). pH-responsive interpenetrating network hydrogel beads of poly(acrylamide)-g-carrageenan and sodium alginate for intestinal targeted drug delivery: Synthesis, in vitro and in vivo evaluation. *Journal of Colloid and Interface Science*, *367*, 509–517.

Rajendran, K., & Sivalingam, T. (2013). Industrial method of cotton fabric finishing with chitosan–ZnO composite for anti-bacterial and thermal stability. *Industrial Crops and Products*, *47*, 160–167.

Rao, K. S. V. K., Naidu, B. V. K., Subha, M. C. S., & Aminabhavi, T. M. (2006). Novel chitosan-based pH-sensitive interpenetrating network microgels for the controlled release of cefadroxil. *Carbohydrate Polymers*, *66*, 333–344.

Ritger, P. L., & Peppas, N. A. (1987). A simple equation for description of solute release I Fickian and non-Fickian release from non-swellable devices in the form of slabs, spheres, cylinders or discs. *Journal of Controlled Release*, *5*, 23–36.

Rokhade, A. P., Shelke, N. B., Patil, S. A., & Aminabhavi, T. M. (2007). Novel interpenetrating polymer network microspheres of chitosan and methylcellulose for controlled release of theophylline. *Carbohydrate Polymers*, *69*, 678–687.

Samanta, H. S., & Ray, S. K. (2014). Synthesis, characterization, swelling and drug release behavior of semi-interpenetrating network hydrogels of sodium alginate and polyacrylamide. *Carbohydrate Polymers*, *99*, 666–678.

Shim, J. W., & Nho, Y. C. (2003). γ-Irradiation preparation of poly(acrylic acid)–chitosan hydrogels for *in vitro* drug release. *Journal of Applied Polymer Science*, *90*, 3270–3277.

Sionkowska, A. (2011). Current research on the blends of natural and synthetic polymers as new biomaterials: Review. *Progress in Polymer Science*, *36*, 1254–1276.

Sokker, H. H., Abdel Ghaffar, A. M., Gad, Y. H., & Aly, A. S. (2009). Synthesis and characterization of hydrogels based on grafted chitosan for the controlled drug release. *Carbohydrate Polymers*, *75*, 222–229.

Sullad, A. G., Manjeshwar, L. S., & Aminabhavi, T. M. (2010a). Controlled release of theophylline from interpenetrating blend microspheres of poly(vinyl alcohol) and methyl cellulose. *Journal of Applied Polymer Science*, *116*, 1226–1235.

Sullad, A. G., Manjeshwar, L. S., & Aminabhavi, T. M. (2010b). Polymeric blend microspheres for controlled release of theophylline. *Journal of Applied Polymer Science*, *117*, 1361–1370.

Sun, L. P., Du, Y. M., Fan, L. H., Chen, X., & Yang, J. H. (2006). Preparation, characterization and antimicrobial activity of quaternized carboxymethyl chitosan and application as pulp-cap. *Polymer*, *47*, 1796–1804.

Tomić, S. Lj., Mićić, M. M., Filipović, J. M., & Suljovrujic, E. H. (2007). Swelling and drug release behavior of poly(2-hydroxyethyl methacrylate/itaconic acid) copolymeric hydrogels obtained by gamma irradiation. *Radiation Physics and Chemistry*, *76*, 801–810.

Tracy, J. W., & Webster, L. T., Jr. (1996). Drugs used in the Chemotherapy of protozoal infections. In J. G. Aardman, A. Goodman, L. Gilman, & E. Limbird (Eds.), *Goodman and Gilman's the pharmacological basis of therapeutics* (10th edition, pp. 1069–1086). USA: McGraw-Hill.

Vaghani, S. S., Patel, M. M., & Satish, C. S. (2012). Synthesis and characterization of pH-sensitive hydrogel composed of carboxymethyl chitosan for colon targeted delivery of ornidazole. *Carbohydrate Research*, *347*, 76–82.

Wang, S. G., Sun, X. F., Liu, X. W., Gong, W. X., Gao, B. Y., & Bao, N. (2008). Chitosan hydrogel beads for fulvic acid adsorption: Behaviors and mechanisms. *Chemical Engineering Journal*, *142*, 239–247.

Wang, W., & Wang, A. (2010). Synthesis and swelling properties of pH-sensitive semi-IPN superabsorbent hydrogels based on sodium alginate-g-poly(sodium acrylate) and polyvinylpyrrolidone. *Carbohydrate Polymers*, *80*, 1028–1036.

Yanga, J., Chena, J., Pana, D., Wanc, Y., & Wang, Z. (2013). pH-sensitive interpenetrating network hydrogels based on chitosan derivatives and alginate for oral drug delivery. *Carbohydrate Polymers*, *92*, 719–725.

Yue, Y., Sheng, X., & Wang, P. (2009). Fabrication and characterization of microstructured and pH sensitive interpenetrating networks hydrogel films and application in drug delivery field. *European Polymer Journal*, *45*, 309–315.

Zhang, J., Wang, Q., & Wang, A. (2007). Synthesis and characterization of chitosan-g-poly(acrylic acid)/attapulgite superabsorbent composites. *Carbohydrate Polymers*, *68*, 367–374.

Zhang, X. Z., Wu, D. Q., & Chu, D. Q. (2004). Synthesis, characterization and controlled drug release of thermosensitive IPN–PNIPAAm hydrogels. *Biomaterials*, *25*, 3793–3805.

Zhou, H. Y., Zhang, Y. P., Zhang, W. F., & Chen, X. G. (2011). Biocompatibility and characteristics of injectable chitosan-based thermosensitive hydrogel for drug delivery. *Carbohydrate Polymers*, *83*, 1643–1651.